International Journal of
Agriculture, Environment and Food Sciences
e-ISSN: 2618-5946 https://dergipark.org.tr/jaefs

DOI: https://doi.org/10.31015/2025.4.13 Int. J. Agric. Environ. Food Sci. 2025; 9 (Special): xxx-xxx

Nano ZnO-Doped Sweet Basil-Based Activated Carbon Electrodes for Supercapacitors

Mehmet Fırat BARAN[1] , Erdal ERTAŞ[2], Abdulkadir LEVENT[3]

[1,2]Department of Food Technology, Vocational School of Technical Sciences, Batman University, Batman, 72100, Türkiye
[3]Batman University, Faculty of Arts and Sciences, Department of Chemistry, Batman, 72100, Türkiye

Article History
Received: October 15, 2025
Accepted: November 30, 2025
Published Online: December 11, 2025

Article Info
Type: Research Article
Subject: Transgenesis

Corresponding Author
Mehmet Fırat Baran
mfiratbaran@gmail.com

Author ORCID
[1]https://orcid.org/0000-0001-8133-6670
[2]https://orcid.org/0000-0002-0325-1257
[3]https://orcid.org/0000-0001-5792-419X

Available at
https://dergipark.org.tr/jaefs/issue/93363/1803978

Abstract

The production of highly efficient and cost-effective electrode materials is critical for the performance of energy storage systems, and therefore nanocomposite materials are ideal candidates for supercapacitor applications. In this study, the synthesis, characterization and electrochemical behavior of SBAC@ZnO nanocomposite obtained by modifying activated carbon (AC) synthesized by activating Sweet Basil (SB) plant with ZnO were investigated in detail. The structural and morphological properties of the SBAC nanocomposite were analyzed using UV-Vis spectroscopy, Fourier transform infrared spectroscopy (FTIR), scanning electron microscopy (SEM), energy dispersive X-ray spectroscopy (EDX), and X-ray diffraction (XRD) techniques. The results indicate that the ZnO particles exhibit a homogeneous distribution on the SBAC surface and support the functionalization of organic functional groups derived from SB. Electrochemical performance evaluations were conducted using cyclic voltammetry (CV), galvanostatic charge-discharge (GCD), and electrochemical impedance spectroscopy (EIS) techniques. In CV analyses, the specific capacitance values of the SBAC and SBAC@ZnO electrodes in Na_2SO_4 electrolyte were obtained as 102.56 F/g and 229.96 F/g, respectively. In GCD experiments, the SBAC@ZnO electrode achieved a substantial Csp value of 426.66 F/g at a current density of 0.1 A/g. The EIS study revealed equivalent series resistance (ESR) values of 48.52 Ω for SBAC and 29.32 Ω for SBAC@ZnO, with charge transfer resistances (Rct) measured at 4.20 Ω and 3.28 Ω, respectively. The results demonstrate that ZnO doping diminishes internal resistance at the electrode-electrolyte interface, enhances ion transport, and optimizes electrochemical kinetics. Bode phase analyses indicated phase angles of 54.46° and 67.65° for SBAC and SBAC@ZnO electrodes, respectively, showing that ZnO doping enhances capacitive behavior. In the low-frequency region, the SBAC electrode reached a capacitance of 161.20 F/g, while the SBAC@ZnO reached a capacitance of 241.61 F/g. The findings indicate that ZnO doping significantly improves electrochemical performance, making the SBAC@ZnO nanocomposite a promising electrode material for supercapacitor applications.

Keywords: Plant-Based Nanomaterial, SBAC@ZnO nanocomposite, Supercapacitors, Galvanostatic charge-discharge, Cyclic voltammetry

Cite this article as: Baran, M.F., Ertas, E., Levent, A. (2025). Nano ZnO-Doped Sweet Basil-Based Activated Carbon Electrodes for Supercapacitors. International Journal of Agriculture, Environment and Food Sciences, 9 (Special): xxx–xxx. https://doi.org/10.31015/2025.4.13

INTRODUCTION

Increasing energy demand, the depletion of fossil fuel reserves, and the negative environmental impacts of these sources have rapidly increased interest in sustainable energy solutions. Renewable energy sources, particularly solar, wind, and wave energy, while providing environmental sustainability, pose challenges in ensuring a continuous energy supply due to their inherent intermittency. Given this, the development of energy storage technologies with high efficiency and long cycle stability is of paramount importance. Supercapacitors play a key role in energy storage technologies with their high power density, rapid charge-discharge capabilities, long cycle life, and low maintenance requirements (Li et al., 2022; Qiu et al., 2018; Özpınar et al., 2022).

Supercapacitors offer high power and energy densities, as well as rapid charge-discharge capabilities, overcoming the limitations of traditional capacitors and batteries. Current research focuses on improving the electrochemical performance

of these devices, increasing their specific capacitance, and optimizing electrode design and device configurations (Chatterjee and Nandi, 2021; Olabi et al., 2022; Yaseen et al., 2021). Supercapacitors are divided into three main classes based on their energy storage mechanisms: electrical double-layer capacitors (EDLCs), pseudocapacitors, and hybrid capacitors (Mallick et al., 2025). EDLCs store charges via physical adsorption, while pseudocapacitors offer higher specific capacitance values due to fast and reversible redox reactions on the electrode surface. Hybrid capacitors aim to provide high power and energy density by combining the advantages of both mechanisms (Kumar et al., 2022b; Rudra et al., 2024). Due to these electrochemical differences, pseudocapacitors generally exhibit higher specific capacitance values compared to EDLC-based materials (Huang et al., 2020).

The performance of supercapacitors depends largely on the design and properties of the electrode materials used. Traditionally, materials with high surface area, such as carbon nanotubes, graphene, and activated carbon, have been preferred. However, the high production costs, environmental impacts, and scalability challenges of these materials necessitate the search for more sustainable and economical alternatives. In this context, biomass-derived carbon components have attracted considerable interest in recent years (Mehdi et al., 2023; Luo et al., 2022; Mandal et al., 2023).

Biomass-derived carbon materials offer attractive alternatives for sustainable energy applications due to their affordable cost, widespread availability, carbon-neutral composition, and environmentally friendly properties. These carbon components are obtained by the controlled pyrolysis or activation of plant waste and generally offer advantages such as high porosity and large surface area (Yasin et al., 2021).

Sweet Basil (*Ocimum basilicum*), a widely cultivated aromatic plant belonging to the Lamiaceae family, was used as a carbon precursor. Its high carbon content and low inorganic residue increase the usability of biochar derived from this plant in energy applications. Furthermore, activated carbon derived from this plant, with its porous structure and surface functional groups, stands out as a promising material in electrochemical energy storage systems (Divani et al., 2017; Solmaz et al., 2024).

Activated carbon obtained from the SB plant via pyrolysis has been evaluated as an electrode material used in supercapacitors when combined with zinc oxide (ZnO) nanoparticles. ZnO, a metal oxide known for its high electrochemical activity, environmentally friendly composition, and economic viability, can exhibit shortcomings such as low conductivity and cycling stability when used alone. Combining ZnO with carbon-based materials overcomes these shortcomings, enabling the simultaneous realization of both bilayer and pseudocapacitive behavior (Yadav et al., 2025; Habib et al., 2025).

The combination of zinc oxide and biochars in supercapacitors has been the subject of limited studies. The aim of this research is to investigate the synthesis, characterization, and electrochemical performance of the electrode material produced using SBAC@ZnO nanocomposites derived from activated carbon obtained from the Sweet Basil plant. The study will evaluate the specific capacitance, cycle life, and conductivity properties of this composite. Such studies may enable the development of environmentally friendly and economical electrode designs.

MATERIALS AND METHODS

Preparation of the SBAC Material

The SB plant stems, branches, and leaves, considered waste, were first washed several times with tap water to remove coarse dirt and particles from their surfaces. Following this process, the samples were thoroughly cleaned using deionized water to completely remove fine dust and other contaminants adsorbed to the surface textures. After the cleaning process, the stems, branches and leaves of the SB plant dried at room temperature were ground into powder using the IKA M20 Universal grinder and stored in a container for use in SBAC production. After drying the SB plant stems, branches and leaves, 40 g of the resulting powder was weighed and transferred to a 300 mL Erlenmeyer flask. A 0.5 M zinc chloride solution (for activated carbon activation) was added and stirred in a shaking water bath at 90°C for 5 hours. After the mixture was cooled to room temperature, the cooled precipitate was transferred to a glass crystallization vessel to achieve a homogeneous structure and dried in an oven at 130°C for 48 hours. Following drying, the resulting solid material was removed from porcelain crucibles and subjected to carbonization in a muffle furnace set at 550°C. The resulting SBAC was cooled in a desiccator at 25°C, ready for storage and subsequent analysis. To remove unreacted zinc, chlorine, and other ions from the SBAC surface, the material was washed several times with 0.1 N HCl solution. Following this acid wash, the product was rinsed with deionized water until the pH was neutralized. Finally, the cleaned material was dried in a 95°C oven for 24 hours before being prepared for analysis and use (Ertaş et al., 2025; Baran et al., 2024).

Preparation of SBAC@ZnO Nanocoposite

As reported in the literature, nanoparticles (NPs) were synthesized by surface coating AC obtained from the SB plant by applying certain modifications (Inbaraj et al., 2021). For this purpose, a 0.5 M zinc nitrate solution was prepared in a volume of 250 mL. Then, 3 g of the previously synthesized SBAC was taken and subjected to reflux in the zinc nitrate solution at 95 °C for 6 hours. After reflux, 0.1 M NaOH solution was added dropwise to reach the pH of the medium to 9.5, and precipitation occurred in approximately two hours. The resulting mixture was separated by centrifugation, and the solid phase was dried in an oven at 110 °C for 48 hours. After drying, the material was subjected to calcination in a muffle furnace at 400 °C. Finally, the synthesized NPs were stored at +4 °C for use in experimental studies (Baran and Ertaş, 2025; Ertaş et al., 2025).

Electrode Preparation

SBAC and SBAC@ZnO electrode materials were prepared using bioactive compounds derived from the SB plant. During the electrode design process, SBAC and SBAC@ZnO were used as active materials, with graphite powder added to increase electrical conductivity and mineral oil as a binder. These three components were carefully mixed in a 7.5:0.5:2 ratio by mass and processed until a homogeneous, paste-like structure was obtained (Levent and Saka, 2025a; Saka and Levent,

2025; Levent and Saka, 2025b). The prepared composite mixture was manually applied to the carbon paste electrode (CPE; MF-2010, BASi) and carefully pressed to ensure smoothness of the electrode surface. This method ensured good adhesion and homogeneous material distribution on the electrode surface, creating a stable and conductive structure for electrochemical measurements.

Electrochemical Measurements

An AUTOLAB PGSTAT128N model potentiostat/galvanostat system was utilized for each and every electrochemical characterisation study that was conducted. The measurements were carried out in a three-electrode cell system manufactured by BASi. The platinum wire (MF-1032, BASi) was utilized as an auxiliary electrode, and the Ag/AgCl (3 M KCl) was utilized as a reference electrode (MF-1063, BASi). Aspects of experimentation and through the utilization of cyclic voltammetry (CV), galvanostatic charge-discharge (GCD), and electrochemical impedance spectroscopy (EIS) techniques, a comprehensive investigation was conducted to examine the electrochemical characteristics of SBAC and SBAC@ZnO based electrodes in a Na2SO4 electrolyte with a concentration of 1 M. To evaluate the intrinsic resistance and diffusion properties linked to the charge storage behavior of the electrode material, EIS measurements were performed at open circuit voltage on the fully discharged electrode. These measurements were carried out in order to determine the behavior of the electrode material. During these experiments, a sinusoidal voltage signal with an amplitude of 10 millivolts was applied in order to scan a large frequency spectrum that contained frequencies ranging from 100 kilohertz to 0.01 Hz.

Calculation of Specific Capacitance

To evaluate the performance of SBAC and SBAC@ZnO materials in energy storage applications, specific capacitance (C_{sp}) values were determined by three different electrochemical methods: CV, GCD and EIS. The calculations of Csp values for each technique were based on the following equations reported in the literature. (Ratha and Samantara, 2018).

1. From CV measurements: $\mathrm{Csp} = \frac{A}{2r\Delta Vm}$
2. From GCD curves: $\mathrm{Csp} = \frac{It_d}{\Delta Vm}$
3. From EIS data: $Csp = \frac{-1}{2\pi fmZ''}$

In addition to specific capacitance, energy density (E_s, in $Whkg^{-1}$) and power density (P_s, in Wkg^{-1}) were calculated using the following relations:

4. $Es\ (Whkg^{-1}) = \frac{\Delta VxIxt_c}{2}$
5. $Ps\ (Wkg^{-1}) = \frac{\mathrm{Es}}{t_d}$

where: A: Area under the CV curve (A·V), r: Potential scan rate ($V \cdot s^{-1}$), ΔV: Potential window (V), I: Discharge current (A), td and tc: Discharge and charge time (s), respectively, m: Mass of the active electrode material (g), f: Frequency (Hz), Z": Imaginary part of impedance (Ω).

RESULTS AND DISCUSSION

UV-Vis Analysis

The optical characteristics of SBAC@ZnO nanoparticles were examined utilizing the UV-visible light spectrum, as depicted in Figure 1. Figure 1 illustrates that SBAC@ZnO nanoparticles exhibit significant absorption at 324 nm, mostly associated with the inherent band absorption of ZnO nanomaterials (Fayazi, 2024; Ding et al., 2020). Absorbance at 324 nm is a key parameter for understanding the optical properties of ZnO nanoparticles. ZnO is a semiconductor material with a wide band gap (approximately 3.37 eV), making it sensitive to UV light. This ability to absorb light in the UV region is a determining factor in the effectiveness of ZnO nanoparticles in photocatalytic, optical, and biomedical applications. 324 nm is the wavelength at which ZnO's electrons transition from the valence band to the conduction band. This transition underlies their photocatalytic activity as well as other optical and biological interactions (Raha and Ahmaruzzaman, 2022; Sulciute et al., 2021).

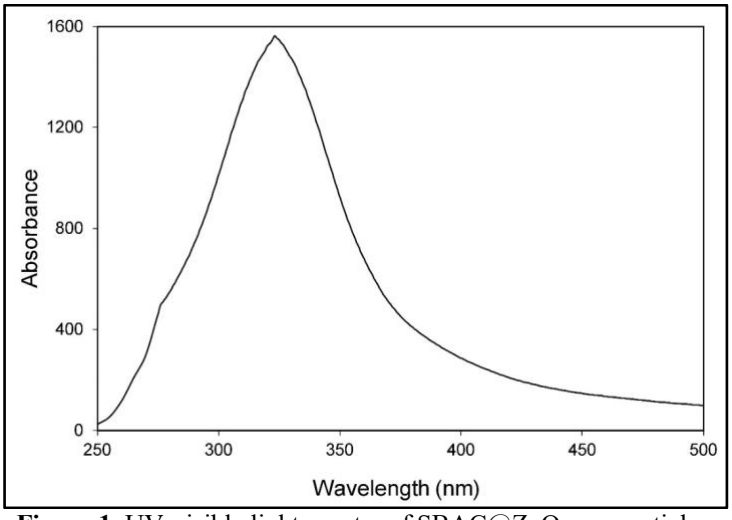

Figure 1. UV-visible light spectra of SBAC@ZnO nanoparticles.

FTIR Analysis

FTIR spectra can provide valuable information about the chemical composition of materials. Since experimental studies have determined that the SBAC@ZnO nanocomposite exhibits the best capacitor properties, the FTIR spectrum of the SBAC@ZnO NP sample was evaluated. Figure 2 shows the FTIR spectrum of the SBAC@ZnO nanocomposite. The weak broad absorption band between 3200 and 3500 cm^{-1} can be attributed to the stretching vibration peak of a hydroxyl group (–OH) of intramolecular bonds (Dai et al., 2018), the peak at 2322 cm^{-1} is attributed to the C=N stretching, 1796 cm^{-1} is associated with the –C=O stretching vibration of carboxylic acid or an acid halide, the signal at 1595 cm^{-1} is the –C=C– of alkene (Daffalla et al., 2020). The peaks at 711 and 872 cm^{-1} in the ZnO band are associated with the stretching vibration of metal-oxygen (Zn-O) and out-of-plane bending peaks of C-H or O-H groups resulting from the doping of SBAC. The peak at 1036 cm^{-1} is attributed to the aromatic ring vibration, which is generally common in carbonaceous materials (Baran et al., 2024; Öziç et al., 2024; Dada et al., 2022).

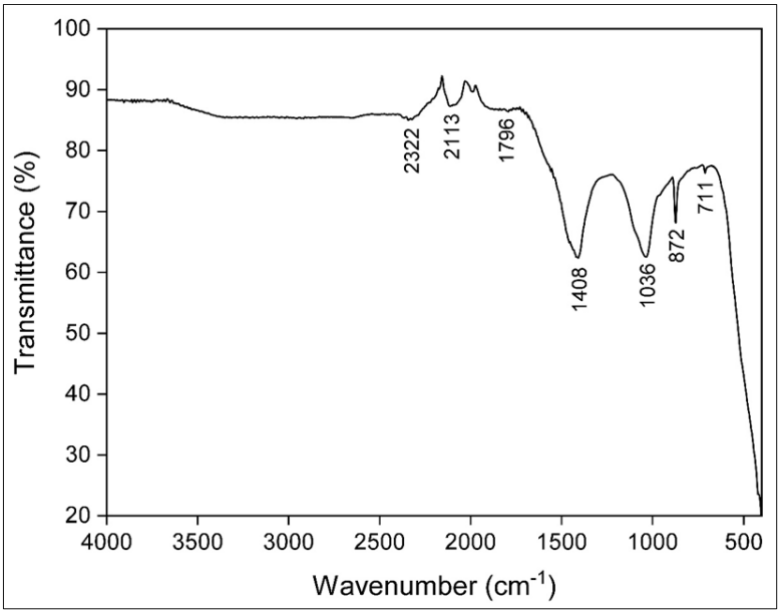

Figure 2. FTIR analysis of SBAC@ZnO nanoparticles.

SEM Analysis

Figure 3 shows the SE image of SBAC@ZnO nanoparticles. The SEM image confirms that the SBAC@ZnO nanocomposite was effectively synthesized by successfully loading the ZnO nanoparticles into the SBAC matrix. The amorphous structure observed in the image (supported by XRD analysis) reflects the porous and irregular surface morphology, high surface area, and porosity. These morphological features, based on the SEM images, indicate that the ZnO nanoparticles are relatively well dispersed in the carbon matrix. It is concluded that these surface morphology, high surface area, and porosity offer high performance potential in photocatalytic, adsorption, and environmental applications, and are highly suitable for electrode fabrication by providing good capacitance(Selvakumar et al., 2010).

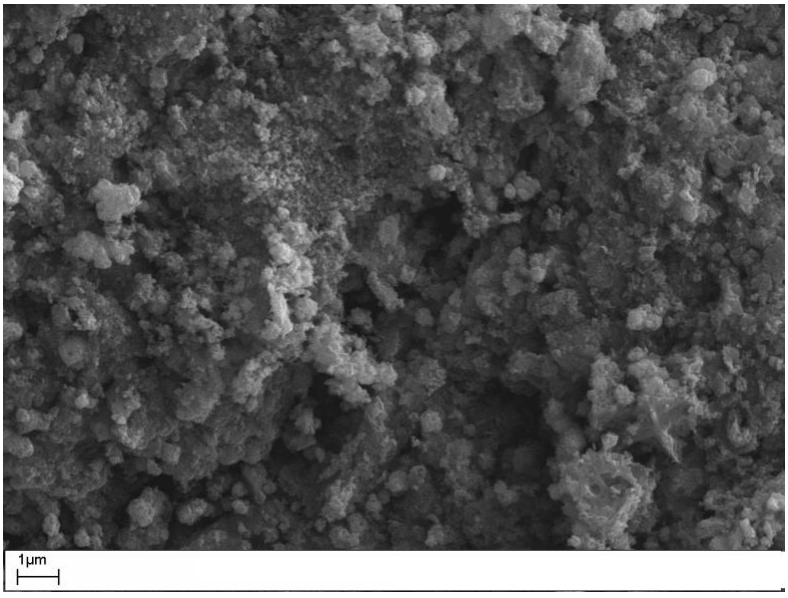

Figure 3. SEM analysis of SBAC@ZnO nanoparticles.

EDX Analysis

Figure 4 shows the presence of C, O, and Zn components in SBAC@ZnO nanoparticles by EDX analysis. The surface elemental composition of SBAC@ZnO nanoparticles was measured as Zn 16.97%, C 37.43%, O 45.15%, P 0.19%, and S 0.25%. When the results were examined, spectral analysis of SBAC@ZnO nanoparticles revealed that zinc (Zn) had absorption peaks at approximately 1-1.25 keV and 8.5-8.75 keV. On the other hand, carbon (C) had optical absorption peaks at 0-0.5 keV and oxygen (O) at 0-0.75 keV. Additionally, elemental mapping images show that zinc and oxygen are homogeneously distributed in the sample and the synthesized SBAC@ZnO nanoparticles are free of impurities (El-Khawaga, et al., 2025; Güneş et al., 2025).

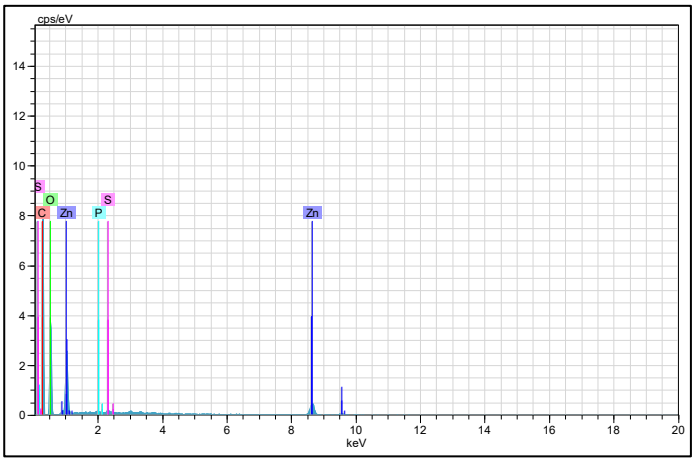

Figure 4. EDX spectrum of SBAC@ZnO nanoparticles.

XRD Analysis

The crystal phase purity and structure of SBAC@ZnO NPs synthesized after the production of activated carbon using SB plant were analyzed by powder XRD analysis. Figure 5 shows that the diffraction peaks are located at 31.66°, 34.30°, 36.16°, 47.48°, 56.54°, 62.76°, 67.96°, and 69.02°, and are consistent with the typical crystal planes (100), (002), (101), (102), (110), (103), (112), and (201) and have a hexagonal structure. These synthesized SBAC@ZnO nanoparticles are in line with the JCPDS Card No. 36–1451 reported in the literature. (Kumar et al., 2022a). Furthermore, the crystal size of the synthesized SBAC@ZnO nanoparticle was calculated using the Scherrer equation (Azizi et al., 2024).

$$D=\frac{K\lambda}{\beta\cos\theta}$$

where D - Particle size of nanoparticles

K - Scherrer constant, s

λ - X-ray wavelength

β - Additional peak width with half peak height

θ - Bragg angle

As a result of the calculation with this equation, the crystal size of the SBAC@ZnO nanoparticle was measured as 27.96 nm. The crystallinity of the synthesized SBAC@ZnO nanoparticle was confirmed by the narrow peak. The XRD pattern showed no other impurity peaks, indicating that the SBAC@ZnO nanoparticles were prepared in pure form.

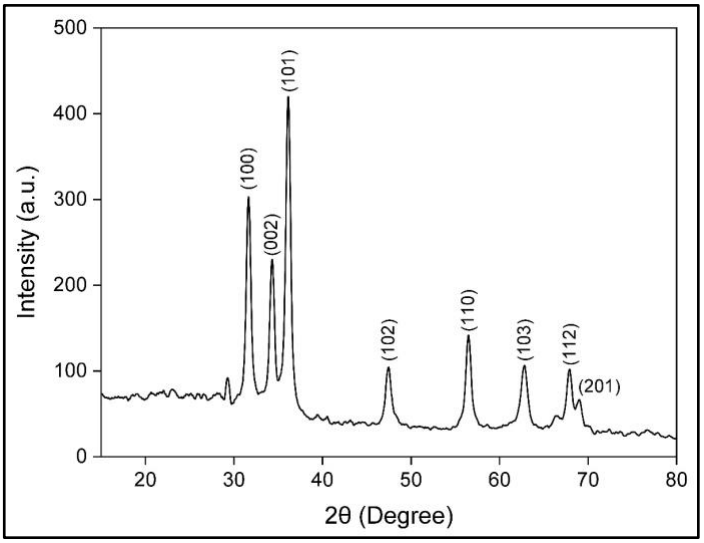

Figure 5. XRD pattern of SBAC@ZnO nanoparticles

Cyclic Voltammetry Results

SBAC@ZnO obtained from SB biomass activated carbon and a ZnO-doped composite electrode were investigated using the CV method in a 1 M Na_2SO_4 electrolyte. Figure 6a shows the CV curves recorded at a scan rate of 5 mV/s, and it was determined that both electrodes exhibited nearly rectangular symmetric profiles. This indicates that the system has a predominantly capacitive character. However, considering the Csp values, the calculated value of 102.56 F/g for SBAC reached 229.96 F/g for the ZnO-doped SBAC@ZnO nanocomposite. This nearly two-fold increase indicates that the ZnO doping improves the electrode structure, facilitates ion transfer, and significantly increases charge storage capacity. The presence of ZnO accelerates ion diffusion by creating additional active centers within the carbon matrix and increases electron conductivity, creating a synergistic effect at the electrode/electrolyte interface (Wu et al., 2021; George et al., 2024; Saka and Levent, 2024).

Figure 6b presents the CV curves and calculated Csp values obtained for SBAC@ZnO electrodes at different scan rates (5–100 mV/s). The maximum Csp value, which was 229.96 F/g at 5 mV/s, gradually decreased with increasing scan rates, reaching 75.69 F/g at 100 mV/s. This tendency is due to the inability of ions to fully diffuse into the electrode pores at high scan rates (Costentin and Savéant, 2019; Levent and Saka, 2024). In contrast, the high Csp values obtained at low scan rates indicate that ions can access the porous structure more effectively. The fact that ZnO-doped electrodes maintain their high capacitive behavior even at different scan rates is a clear indication of the advantage ZnO provides to the electrode structure (Levent and Saka, 2024; Guo et al., 2021; Abbas et al., 2021; Saka and Levent, 2024).

The results obtained are quite striking compared to similar studies reported in the literature. For example, ZnO-modified carbon-based electrodes have generally been reported to exhibit Csp values in the range of 150–200 F/g. (Tang et al., 2021; Li and Liu, 2014; Sasirekha et al., 2018; Zhu et al., 2025). In this study, the high capacitance of 229.96 F/g achieved by the ZnO-doped SBAC@ZnO electrodes clearly demonstrates the suitability of the porous structure of biomass-based carbon and the synergistic contribution provided by ZnO. Therefore, the high capacitance values and stable electrochemical performance of the ZnO-doped SBAC@ZnO electrodes make them strong candidates for high-efficiency energy storage applications.

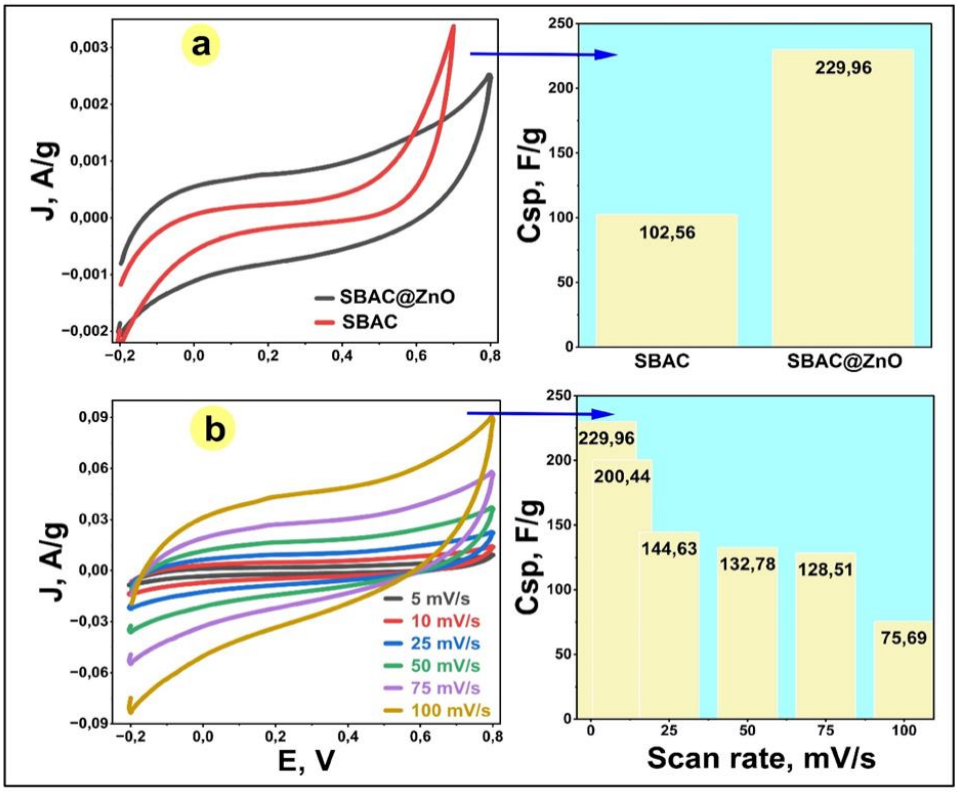

Figure 6. (a) CV curves of SBAC and SBAC@ZnO electrodes recorded at a scan rate of 5 mV s^{-1}; (b) CV profiles of the SBAC@ZnO electrode at various scan rates together with the corresponding specific capacitance values.

Galvanostatic Charge–Discharge Results

The electrochemical performance of SBAC@ZnO hybrid electrodes obtained from SB biomass was evaluated by GCD measurements. Figure 7 presents the GCD curves recorded at different current densities and the corresponding Csp values. The symmetric and triangular profiles of the curves indicate that the electrode material exhibits a typical electrochemical double-layer capacitor (EDLC) behavior, thus predominating reversible adsorption–desorption processes of ions on the surface. The hybrid electrode exhibited a high Csp value of 426.66 F/g at a current density of 0.1 A/g. A gradual decrease in Csp values was observed with increasing current densities due to the limitation of ion diffusion. This performance is due not only to the large surface area and porous morphology of the activated carbon, but also to the heterogeneous active centers formed by the ZnO doping. ZnO increased the charge storage capacity by allowing ions to adhere more effectively to the

electrode surface, providing a significant advantage over pure carbon-based electrodes (Xiao et al., 2017; George et al., 2024).; Saka and Levent, 2024; Levent and Saka, 2024; Ercay et al., 2025).

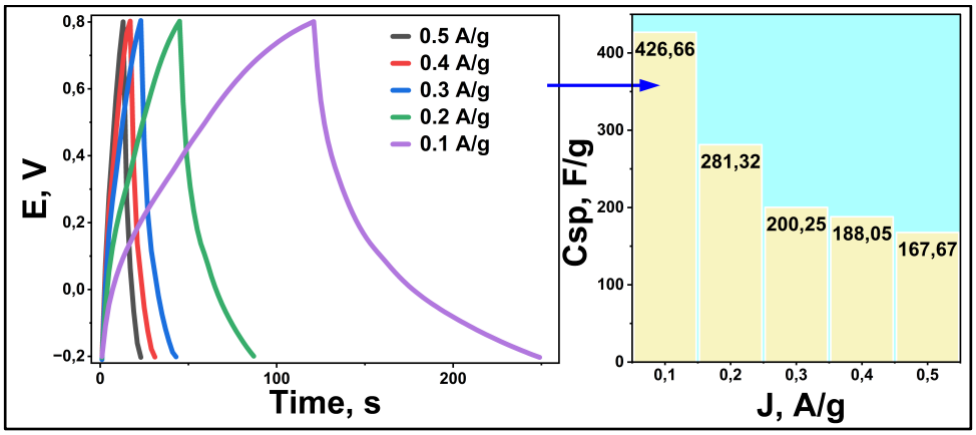

Figure 7. Different current densities galvanostatic charge–discharge curves of the SBAC@ZnO electrode and the corresponding specific capacitance values.

Cycle stability evaluations were performed for 5000 GCD cycles in a 1 M Na_2SO_4 electrolyte at a current density of 0.5 A/g. Figure 8 indicates that the approximately 92.16% Csp retention unequivocally illustrates the intrinsic resistance and elevated electrochemical reversibility of the electrode material. The maintenance of the symmetric triangular shape of the GCD curves for the initial and final 10 cycles verifies that the EDLC properties remain consistent after prolonged cycling. The elevated Coulombic efficiency and retention of capacitance stem from the synergistic influence of ZnO doping inside the carbon matrix and its surface reactivity (Anandhi et al., 2024; George et al., 2024; Saka and Levent, 2024; Levent and Saka, 2024; Wang et al., 2012). The presence of ZnO suppresses the tendency for deterioration or passivation on the electrode surface, thus providing high durability in long-term operations.

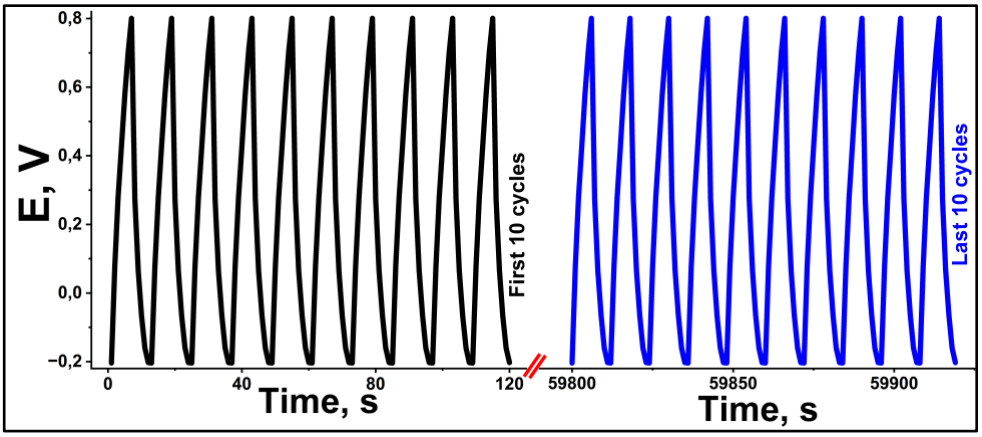

Figure 8. Coulombic efficiency data of SBAC@ZnO supercapacitor 1 M Na_2SO_4 media for 5000 cycles.

The energy storage characteristics of the SBAC@ZnO hybrid electrodes were assessed utilizing the Ragone curve (Figure 9). The results from the 1 M Na_2SO_4 electrolyte indicated that the device attained an energy density of roughly 8.17 Wh/kg at a low power density of 675 W/kg. As the power density rose to 1870 W/kg, the energy density diminished to 3.90 Wh/kg. This trend validates the inverse correlation between elevated power density and diminished energy density, a distinguishing hallmark of supercapacitors. Nonetheless, the ZnO doping alleviates this inverse trend, enabling the device to sustain considerable energy density even at elevated power densities. The supplementary active sites generated by ZnO enhance ion transport and promote charge transfer, hence achieving a favorable standing on the Ragone curve (Levent and Saka, 2024; George et al., 2024; Wu et al., 2021; Saka and Levent, 2024). Thus, the device can maintain significant energy density even under high power density conditions. This position observed in the Ragone curve demonstrates that ZnO-doped electrodes are a competitive and promising candidate for energy storage devices.

Electrochemical Impedance Spectroscopy Analysis

The electrochemical properties of the SBAC and SBAC@ZnO electrodes were investigated using EIS measurements, and the results are presented in Figure 10. Nyquist curves (Figure 10a) reveal the series resistance contribution in the high-frequency region and the typical capacitive behavior in the low-frequency region for both electrodes. The calculated equivalent series resistance (ESR) values in the Na_2SO_4 electrolyte medium were found to be 48.52 Ω for the SBAC and 29.32 Ω for the ZnO-doped SBAC@ZnO electrode. This result indicates that the ZnO doping provides lower internal resistance at the electrode-electrolyte interface and facilitates ion transport. (Kumar et al., 2023; Zhang and Pan, 2015). Charge transfer resistances (Rct) were calculated as 4.20 Ω for SBAC and 3.28 Ω for SBAC@ZnO. The decrease in Rct

value due to ZnO doping reveals that it accelerates electron transfer at the electrode surface and improves electrochemical kinetics (Li et al., 2013; George et al., 2024; Wu et al., 2021; Saka and Levent, 2024; Levent and Saka, 2024). Upon analysis of the Bode phase diagrams (Figure 10b), the phase angle for SBAC was recorded at 54.46°, while that for SBAC@ZnO was noted at 67.65°. These values confirm that ZnO doping enhances the electrodes' capacitive performance. The Csp values distinctly demonstrate the influence of ZnO doping on capacitive characteristics (Figure 10c). In the low-frequency range, the SBAC electrode demonstrated a capacitance of 161.20 F/g, whereas the SBAC@ZnO electrode attained a capacitance of 241.61 F/g. This rise signifies that ZnO enhances ion adsorption by augmenting active sites and boosting double-layer capacitance. These findings indicate that ZnO doping enhances internal resistance and charge transfer in the electrodes while reinforcing capacitive behavior, demonstrating that the SBAC@ZnO electrode is a superior choice for supercapacitor applications.

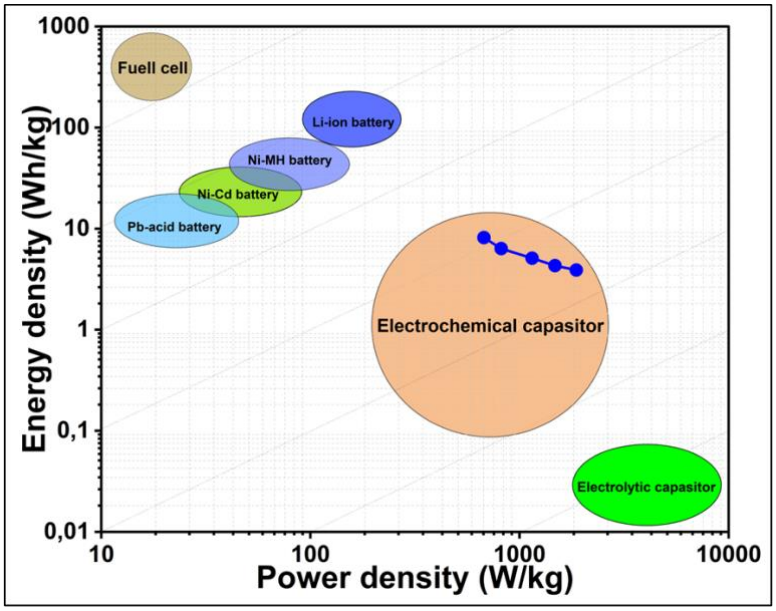

Figure 9. Ragone plot curves of the power and energy densities for SBAC@ZnO supercapacitor

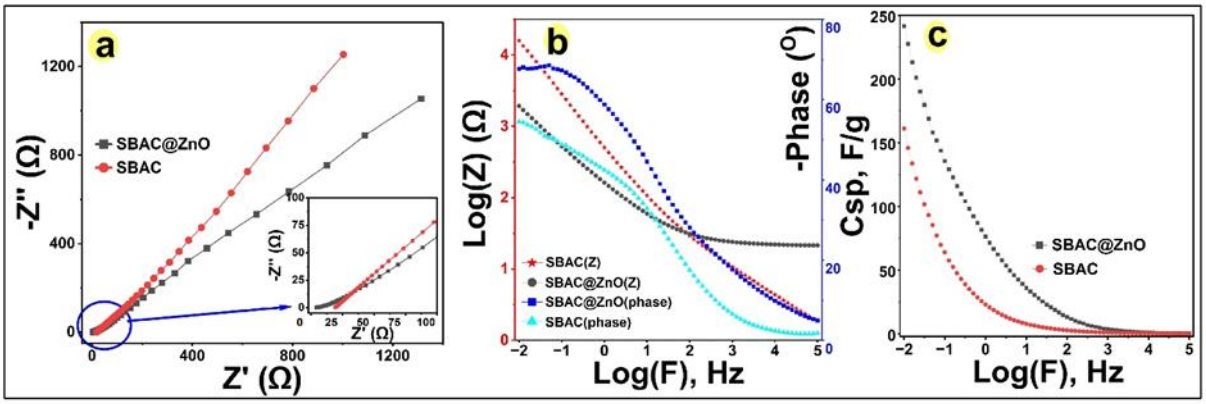

Figure 10. Electrochemical impedance analysis of SBAC@ZnO supercapacitor: (a) Nyquist plots, (b) Bode phase diagrams, and (c) calculated specific capacitance values

CONCLUSION

The properties of the SBAC@ZnO nanocomposite produced using biochar-based activated carbon (SBAC) derived from the SB plant were comprehensively investigated in this study. SBAC, developed through an environmentally friendly and sustainable method, was successfully integrated with ZnO, and the resulting nanocomposite material was evaluated as an electrode for supercapacitor applications. Structural analyses revealed that ZnO nanoparticles were homogeneously distributed on the SBAC surface, and plant-derived functional groups contributed significantly to surface functionalization.

Electrochemical analyses indicate that the addition of ZnO significantly enhances electrode performance. SBAC@ZnO electrodes exhibited high specific capacitance (Csp) values in CV and GCD tests, demonstrating a significant improvement in the energy storage capacity of this material. The Csp value of 426.66 F/g obtained at a current density of 0.1 A/g confirms that the SBAC@ZnO nanocomposite provides a significant performance increase in supercapacitor applications. EIS data reveal that the SBAC@ZnO electrode has lower equivalent series resistance (29.32 Ω) and charge transfer resistance (3.28 Ω), demonstrating the facilitating effect of the ZnO doping on electron and ion transport. Furthermore, the increase in the Bode phase angle and the higher capacitance values obtained in the low-frequency region clearly demonstrate the positive effects of ZnO on capacitive behavior and double-layer capacitance.

The findings indicate that SBAC@ZnO nanocomposite is a suitable candidate for supercapacitor applications as an environmentally friendly, low-cost and high-performance electrode material. Furthermore, it is concluded that the functionalization of plant-derived carbon materials with metal oxides has the potential to provide sustainable and innovative solutions for energy storage systems.

Compliance with Ethical Standards

Peer Review

This article has been reviewed by independent experts in the field using a rigorous double-blind peer review process.

Conflict of Interest

The authors declare that they have no known competing financial interests or personal relationships that could have appeared to influence the work reported in this paper.

Author Contributions

All authors contributed equally to the study design, data collection, analysis, and manuscript preparation.

REFERENCES

Anandhi, P., Harikrishnan, S., Mahalingam, S., Kumar, V. J. S., Lai, W. C., Rahaman, M., & Kim, J. (2024). Efficient and stable supercapacitors using rGO/ZnO nanocomposites via wet chemical reaction. *Inorganic Chemistry Communications*, *166*, 112675. https://doi.org/10.1016/j.inoche.2024.112675

Azizi, S., Askari, M. B., Rozati, S. M., & Masoumnezhad, M. (2024). Nickel ferrite coated on carbon felt for asymmetric supercapacitor. *Chemical Physics Impact*, *8*, 100543. https://doi.org/10.1016/j.chphi.2024.100543

Baran, A., Ertaş, E., Baran, M. F., Eftekhari, A., Gunes, Z., Keskin, C., Khalilov, R. (2024). Green-synthesized characterization, antioxidant and antibacterial applications of CtAC/MNPs-Ag nanocomposites. *Pharmaceuticals*, *17*(6), 772. https://doi.org/10.3390/ph17060772

Baran, A., Ertaş, E. (2025). Preparation, characterization and in vitro applications of morin hydrate loaded HPAC@MNPs nanocomposite. *Journal of the Institute of Science and Technology*, 15(1), 217-227. https://doi.org/10.21597/jist.1533345

Chatterjee, D. P., & Nandi, A. K. (2021). A review on the recent advances in hybrid supercapacitors. Journal of Materials Chemistry A, 9(29), 15880-15918. https://doi.org/10.1039/D1TA02505H

Costentin, C., & Savéant, J. M. (2019). Energy storage: pseudocapacitance in prospect. *Chemical Science*, *10*(22), 5656-5666. https://doi.org/10.1039/C9SC01662G

Ding, C., Fu, K., Pan, Y., Liu, J., Deng, H., & Shi, J. (2020). Comparison of Ag and Agi-modified ZnO as heterogeneous photocatalysts for simulated sunlight driven photodegradation of metronidazole. *Catalysts*, *10*(9), 1097. https://doi.org/10.3390/catal10091097

Divani, S., Paknejad, F., Ghafourian, H., Alavifazel, M., & Ardakani, M. R. (2017). Feasibility Study on Reducing Lead and Cadmium Absorption in *Sweet Basil* (*Ocimum basilicum* L.) With Using Active Carbon. *Journal of Crop Nutrition Science*, *3*(1), 25-36. https://oiccpress.com/jcns/article/view/5847

El-Khawaga, A. M., Elsayed, M. A., Gobara, M., Suliman, A. A., Hashem, A. H., Zaher, A. A., Salem, S. S. (2025). Green synthesized ZnO nanoparticles by Saccharomyces cerevisiae and their antibacterial activity and photocatalytic degradation. *Biomass Conversion and Biorefinery*, 15(2), 2673-2684. https://doi.org/10. 1007/s13399-023-04827-0

Ertaş, E., Doğan, S., Baran, A., Baran, M. F., Evcil, M., Kurt, B., Aslan, K. S. (2025). Preparation and Characterization of Silver-Loaded Magnetic Activated Carbon Produced from Crataegus Monogyna for Antimicrobial and Antioxidant Applications. *ChemistrySelect*, *10*(16), e202405558. https://doi.org/10.1002/ slct.202405558

Fayazi, M. (2024). Synthesis of ZnO nanostructures with different morphologies on biochar support for photocatalytic degradation of organic dye. *Journal of Water and Environmental Nanotechnology*, *9*(2), 137-148. https://doi.org/10.22090/jwent.2024.02.02

George, N. S., Singh, G., Bahadur, R., Kumar, P., Ramadass, K., Sathish, C. I., Vinu, A. (2024). Recent Advances in Functionalized Biomass-Derived Porous Carbons and their Composites for Hybrid Ion Capacitors. *Advanced Science*, *11*(35), 2406235. https://doi.org/10.1002/advs.202406235

Güneş, M., Ertaş, E., Tumur, S., Zulfugarova, P., Nuriyeva, F., Kavetskyy, T., Kukhazh, Y., Grozdov, P., Šauša, O., Smutok, O., Ganbarov, D., & Kiv, A. (2025). Synthesis and Antibacterial Evaluation of Silver-Coated Magnetic Iron Oxide/Activated Carbon Nanoparticles Derived from Hibiscus esculentus. *Magnetochemistry*, 11(7), 53. https://doi.org/10.3390/magnetochemistry11070053

Habib, W., Saji, A., Paul, F., Markapudi, P. R., Wilson, C., & Manjakkal, L. (2025). Flexible electrochemical capacitors based on ZnO-carbon black composite. *Results in Engineering*, *25*, 104510. https://doi.org/10.1016/j.rineng.2025.104510

Huang, T., Jiang, Y., Shen, G., & Chen, D. (2020). Recent advances of two-dimensional nanomaterials for electrochemical capacitors. ChemSusChem, 13(6), 1093-1113. https://doi.org/10.1002/cssc.201903260

Inbaraj, B. S., Sridhar, K., & Chen, B. H. (2021). Removal of polycyclic aromatic hydrocarbons from water by magnetic activated carbon nanocomposite from green tea waste. *Journal of Hazardous Materials*, *415*, 125701. https://doi.org/10.1016/j.jhazmat.2021.125701

Kumar, R. D., Nagarani, S., Balachandran, S., Brundha, C., Kumar, S. H., Manigandan, R., Kim, S. H. (2022a). High performing hexagonal-shaped ZnO nanopowder for Pseudo-supercapacitors applications. *Surfaces and Interfaces*, *33*, 102203. https://doi.org/10.1016/j.surfin.2022.102203

Kumar, N., Kim, S. B., Lee, S. Y., & Park, S. J. (2022b). Recent advanced supercapacitor: a review of storage mechanisms, electrode materials, modification, and perspectives. Nanomaterials, 12(20), 3708. https://doi.org/10.3390/nano12203708

Kumar, S., Ahmed, F., Shaalan, N. M., Arshi, N., Dalela, S., & Chae, K. H. (2023). Influence of Fe Doping on the Electrochemical Performance of a ZnO-Nanostructure-Based Electrode for Supercapacitors. *Nanomaterials*, *13*(15), 2222. https://doi.org/10.3390/nano13152222

Levent, A., & Saka, C. (2024). Enhanced electrochemical performance of ZnO@sulphur-doped carbon particles for use in supercapacitors. *Journal of Energy Storage*, *78*, 110120. https://doi.org/10.1016/j.est.2023.110120

Levent, A., & Saka, C. (2025a). Stable electrode material for use in supercapacitor with iodine doping after sulfonation of mesoporous activated carbon particles based on microalgae biomass. *Biomass Conversion and Biorefinery*, 1-14. https://doi.org/10.1007/s13399-025-06696-1

Levent, A., & Saka, C. (2025b). Tunable energy storage in acidic and alkaline electrolytes using a NiO-embedded N, P-Doped biomass-derived electrode. *Biomass and Bioenergy*, *202*, 108225. https://doi.org/10.1016/ j.biombioe.2025.108225

Li, S., Tan, X., Li, H., Gao, Y., Wang, Q., Li, G., & Guo, M. (2022). Investigation on pore structure regulation of activated carbon derived from sargassum and its application in supercapacitor. *Scientific Reports*, *12*(1), 10106. https://doi.org/10.1038/s41598-022-14214-w

Li, Z., Zhou, Z., Yun, G., Shi, K., Lv, X., & Yang, B. (2013). High-performance solid-state supercapacitors based on graphene-ZnO hybrid nanocomposites. *Nanoscale Research Letters*, *8*(1), 473. https://doi.org/10.1186/ 1556-276X-8-473

Luo, L., Lan, Y., Zhang, Q., Deng, J., Luo, L., Zeng, Q., Zhao, W. (2022). A review on biomass-derived activated carbon as electrode materials for energy storage supercapacitors. *Journal of Energy Storage*, *55*, 105839. https://doi.org/10.1016/j.est.2022.105839

Mallick, S., Bag, S., & Retna Raj, C. (2025). Supercapacitors for energy storage: Fundamentals and materials design. Journal of Chemical Sciences, 137(3), 65. https://doi.org/10.1007/s12039-025-02394-7

Mandal, S., Hu, J., & Shi, S. Q. (2023). A comprehensive review of hybrid supercapacitor from transition metal and industrial crop based activated carbon for energy storage applications. *Materials Today Communications*, *34*, 105207. https://doi.org/10.1016/j.mtcomm.2022.105207

Mehdi, R., Naqvi, S. R., Khoja, A. H., & Hussain, R. (2023). Biomass derived activated carbon by chemical surface modification as a source of clean energy for supercapacitor application. *Fuel*, *348*, 128529. https:// doi.org/10.1016/j.fuel.2023.128529

Olabi, A. G., Abbas, Q., Al Makky, A., & Abdelkareem, M. A. (2022). Supercapacitors as next generation energy storage devices: Properties and applications. Energy, 248, 123617. https://doi.org/10.1016/j.energy. 2022.123617

Öziç, C., Ertaş, E., Baran, M. F., Baran, A., Ahmadian, E., Eftekhari, A., Yıldıztekin, M. (2024). Synthesis and characterization of activated carbon-supported magnetic nanocomposite (MNPs-OLAC) obtained from okra leaves as a nanocarrier for targeted delivery of morin hydrate. *Frontiers in Pharmacology*, 15, 1482130.

Qiu, W., Xiao, H., Yu, M., Li, Y., & Lu, X. (2018). Surface modulation of $NiCo_2O_4$ nanowire arrays with significantly enhanced reactivity for ultrahigh-energy supercapacitors. *Chemical Engineering Journal*, *352*, 996-1003. https://doi.org/10.1016/j.cej.2018.04.118

Raha, S., & Ahmaruzzaman, M. (2022). ZnO nanostructured materials and their potential applications: progress, challenges and perspectives. *Nanoscale Advances*, 4(8), 1868-1925. https://doi.org/10.1039/D1NA00880C

Ratha, S., & Samantara, A. K. (2018). Supercapacitor: instrumentation, measurement and performance evaluation techniques. Springer.

Rudra, S., Seo, H. W., Sarker, S., & Kim, D. M. (2024). Supercapatteries as hybrid electrochemical energy storage devices: current status and future prospects. Molecules, 29(1), 243. https://doi.org/10.3390/ molecules29010243

Saka, C., & Levent, A. (2024). Fabrication of nitrogen and ZnO doped on carbon particles obtained from waste biomass and their use as supercapacitor electrodes for energy storage. *International Journal of Hydrogen Energy*, *90*, 1070-1083. https://doi.org/10.1016/j.ijhydene.2024.10.061

Saka, C., & Levent, A. (2025). Robust and highly mesoporous magnesium oxide and nitrogen atoms incorporated hierarchical porous carbon particles as electrode material for high-performance energy storage in acidic, neutral, and basic electrolytes. *Environmental Science and Pollution Research*, 1-13. https://doi.org/10.1007/ s11356-025-36871-w

Selvakumar, M., Bhat, D. K., Aggarwal, A. M., Iyer, S. P., & Sravani, G. (2010). Nano ZnO-activated carbon composite electrodes for supercapacitors. *Physica B: Condensed Matter*, *405*(9), 2286-2289. https://doi.org/ 10.1016/j.physb.2010.02.028

Solmaz, A., Turna, T., & Baran, A. (2024). Removal of paracetamol from aqueous solution with zinc oxide nanoparticles obtained by green synthesis from *purple basil* (*Ocimum basilicum* L.) waste. *Biomass Conversion and Biorefinery*, *14*(9), 10771-10789. https://doi.org/10.1007/s13399-024-05355-1

Sulciute, A., Nishimura, K., Gilshtein, E., Cesano, F., Viscardi, G., Nasibulin, A. G., Rackauskas, S. (2021). ZnO nanostructures application in electrochemistry: influence of morphology. *The Journal of Physical Chemistry C*, 125(2), 1472-1482. https://doi.org/10.1021/acs.jpcc.0c08459

Wang, G., Zhang, L., & Zhang, J. (2012). A review of electrode materials for electrochemical supercapacitors. *Chemical Society Reviews*, *41*(2), 797-828. https://doi.org/10.1039/C1CS15060J

Wu, C., Zhang, F., Xiao, X., Chen, J., Sun, J., Gandla, D., Ein-Eli, Y., & Tan, D. Q. (2021). Enhanced Electrochemical Performance of Supercapacitors via Atomic Layer Deposition of ZnO on the Activated Carbon Electrode Material. *Molecules*, *26*(14), 4188. https://doi.org/10.3390/molecules26144188

Yadav, R., Sharma, S., Borkar, H., & Kumari, K. (2025). Zinc Oxide-Enhanced Porous Activated Carbon From Waste Walnut Shells for Supercapacitor Electrodes. *Energy Storage*, *7*(3), e70154. https://doi.org/10.1002/ est2.70154

Yaseen, M., Khattak, M. A. K., Humayun, M., Usman, M., Shah, S. S., Bibi, S., Hasnain, B. S. U., Ahmad, S. M., Khan, A., Shah, N., Tahir, A. A., & Ullah, H. (2021). A Review of Supercapacitors: Materials Design, Modification, and Applications. Energies, 14(22), 7779. https://doi.org/10.3390/en14227779

Yasin, A. S., hyun Kim, D., & Lee, K. (2021). One-pot synthesis of activated carbon decorated with ZnO nanoparticles for capacitive deionization application. *Journal of Alloys and Compounds*, *870*, 159422. https:// doi.org/10.1016/j.jallcom.2021.159422

Zhang, S., & Pan, N. (2015). Supercapacitors performance evaluation. *Advanced Energy Materials*, *5*(6), 1401401. https://doi.org/10.1002/aenm.201401401